The Thickness of the Human Precorneal Tear Film: Evidence from Reflection Spectra

P. Ewen King-Smith,[1] *Barbara A. Fink,*[1] *Nick Fogt,*[1] *Kelly K. Nichols,*[1] *Richard M. Hill,*[1] *and Graeme S. Wilson*[2]

Purpose. Interferometric methods have considerable potential for studying the thickness of layers of the human tear film and cornea because of their ability to make noninvasive, accurate, and rapid measurements. However, previous interferometric studies by Prydal and Danjo yielded tear thickness values near 40 and 11 μm, respectively, considerably greater than estimates made by invasive methods of 4 to 8 μm. Using a modified version of Danjo's method, interference effects from the tear film and cornea were studied, with the aim of correlation with known structure and optical properties of the cornea and hence determining the most probable value of tear film thickness.

Methods. Reflectance spectra from the human cornea were measured at normal incidence. These spectra show oscillations whose maxima correspond to constructive interference between light reflected from the air surface and from some deeper surface. The frequency of these spectral oscillations is proportional to the thickness of the layer between the air surface and the second surface. Therefore, Fourier analysis of reflectance spectra can be used to determine the thickness of layers of the tear film and cornea. In the main experiment, 36 low-resolution spectra were obtained from six normal eyes for measuring thickness up to 100 μm. Control experiments included measurements of the time course of thickness changes and high-resolution spectra for measuring thickness up to 1000 μm.

Results. For the main experiment, in the thickness range 1 to 100 μm, the strongest peak in the Fourier transform was near 3 μm (range, 1.5–4.7 μm) beneath the air surface. In the range 20 to 100 μm, the strongest peak was near 55 μm (range, 50–59 μm) for all 36 spectra; none were in Prydal's range near 40 μm. This 55-μm peak is consistent with a reflection from the basement membrane of the epithelium. Time course measurements after a blink show that the 3-μm peak is not an artifact. High-resolution spectra gave a peak near 510 μm, corresponding to the complete thickness of the cornea (plus tear film). This peak had a contrast similar to that of the 3-μm peak.

Conclusions. These studies did not confirm Prydal's estimate of approximately 40 μm. Nor were there prominent peaks near Danjo's value of approximately 11 μm, except in cases of probable reflex tears. Because the reflection at the aqueous–mucus boundary would be expected to be weaker than that from the epithelial surface, the 3-μm peak is unlikely to correspond to the aqueous layer (rather than the complete tear film). The proposal that the 3-μm peak corresponds to a reflection from the *front* of the cornea is supported by the demonstration of a peak of similar contrast from the *back* of the cornea. Thus, the current evidence consistently supports a value of approximately 3 μm for the thickness of the human precorneal tear film. (*Invest Ophthalmol Vis Sci.* 2000;41:3348–3359)

Knowledge of the thickness of the human precorneal tear film is important for an understanding of many fundamental properties, including the quantitative structure of the tear film (e.g., in terms of Wolff's theory of lipid, aqueous, and mucus layers,[1]), the deposition of the tear film by a blink,[2] its redistribution after a blink,[3] and the formation of dry spots.[4] It is therefore unfortunate that estimates of human tear film thickness vary from approximately 4 μm[5] to 40 μm,[6] and there is no consensus on which value is correct.

The first measurements of tear film thickness used methods that potentially disturbed the tear film, such as placing glass fibers against the cornea,[7] measuring fluorescence after instilling fluorescein,[5,7] or applying absorbent paper to the cornea.[8] Such invasive methods have produced thickness estimates for the human tear film between 4 μm[5] and 8 μm.[8] A limitation of these methods is that the invasive nature of the procedure may alter the thickness of the tear film. This could be avoided by using noninvasive methods such as microscopy and interferometry. However, microscopy has not yet been applied with much success to the human tear film; Prydal et

From the [1]College of Optometry, the Ohio State University, Columbus, Ohio; and [2]School of Optometry, Indiana University, Bloomington, Indiana.

Supported by The Ohio Lions Eye Research Foundation, Columbus, Ohio, and John P. Schoessler, College of Optometry, The Ohio State University, Columbus, Ohio.

Submitted for publication February 28, 2000; revised May 16, 2000; accepted May 24, 2000.

Commercial relationships policy: N.

Corresponding author: P. Ewen King-Smith, College of Optometry, The Ohio State University, 338 W. 10th Avenue, Columbus, OH 43210. king-smith.1@osu.edu

al.[6] reported thickness values of 41 to 46 μm using confocal microscopy but noted that images were not sufficiently clear to identify the tear layer with certainty.

The most promising noninvasive method is interferometry.[9] In this method, the intensity of light reflected from the air surface of the tears is modified by interference from light reflected from a deeper surface, such as the corneal surface. (The air surface reflects much more light than other surfaces, and so it is generally one of the two surfaces involved in interference effects.) Maxima and minima of reflected intensity occur when the two reflections are in phase or out of phase, respectively. The tear film thickness can be derived from observation of these maxima and minima (bright and dark fringes) in the reflected light.[9] Interferometric methods are potentially accurate; for example, corneal thickness can be measured by "partial coherence interferometry" with a SD of less than 0.1%.[10] Interferometric measurement of the tear film can be rapid enough to permit video photography.[11]

For the tear film, whose refractive index is intermediate between that of the surrounding air and cornea, maxima of reflectance occur[9,12] when

$$m = 2nt \cos(\phi')/\lambda = 2n\chi t \cos(\phi') = 0, 1, 2\cdots \quad (1)$$

where m is called the order of the maximum, n is the refractive index of the film, t is its thickness, ϕ' is the angle of refraction in the film, λ is the vacuum wavelength, and $\chi = 1/\lambda$ is wave number. Thus, interference fringes depend on three main factors, namely, t, ϕ', and λ. Interference effects can be studied by varying any one of these three factors; correspondingly, the thickness of the tear film has been studied by three methods, which have been called "thickness-dependent fringes," "angle-dependent fringes," and "wavelength-dependent fringes," respectively.[9] Ideally, for any of these methods, one factor is varied while the other two are held constant.[9]

An advantage of thickness-dependent fringes is that they provide a two-dimensional "map" of the thickness of the tear film.[11,13] For the *pre (contact) lens* tear film, bright and dark fringes are seen in front of the lens, which represent contours of tear film thickness. Each cycle corresponds to a thickness difference of $\lambda/2n$. Tear film thickness at any location can be derived by counting the fringes between a dry spot and that location. For the *precorneal* tear film, the observed interference effects correspond to the thin, outer lipid layer.[11,13] Fringes corresponding to complete tear film thickness have not been detected; probably their contrast is too low and is masked by interference effects from the lipid layer.

Angle-dependent fringes have been used to measure human corneal thickness by Green et al.,[14] but they found that fringes from the precorneal tear film were of low contrast and were too thin to quantify; thickness was estimated to be 10 μm or less. However, Prydal's group found tear thickness in the range 34 to 45 μm in six subjects,[6] in reasonable agreement with their confocal microscopy. Application of 20% acetylcysteine, a mucolytic agent, thinned the tear film in one subject to 11 μm, which then returned to a thickness of approximately 40 μm over 40 minutes. They concluded that the precorneal tear film is approximately 40 μm thick and is mainly mucus.

In the method of wavelength-dependent fringes, which is used in this article, a reflection spectrum is measured for a small spot on the cornea at normal incidence. Interference gives rise to "spectral oscillations," maxima and minima in the reflection spectra that are analogous to the bright and dark fringes seen in thickness- and angle-dependent fringes. The thickness of the film is proportional to the frequency of these oscillations.[15,16] Olsen[15] used the principle of this method to interpret his observation that reflectance from the human eye is greater at 500 nm than at 700 nm. He concluded that this difference corresponds to part of a low-frequency spectral oscillation from the lipid layer, which he estimated to be 0.04 μm thick. Danjo et al.[16] applied this method to measuring the complete thickness of the human precorneal tear film, which they found to be 12.0 and 10.3 μm in two subjects. We reported strong (up to 24% contrast) spectral oscillations from the prelens tear film,[17] giving thickness values of up to 4.9 μm, in reasonable agreement with values (up to 4.4 μm) from thickness-dependent fringes.[13] Weak spectral oscillations were recorded from the precorneal tear film of one subject, yielding a thickness of approximately 3 μm.

In this study, a modified version of Danjo's method was used to study interference effects from the tear film and cornea. The purpose was to correlate the findings with the known structure and optical properties of the cornea and the optical properties of the tear film, with the aim of determining the most probable value of tear film thickness. A preliminary report of some of the present study has been made.[18]

METHODS

The optical system is shown in Figure 1A and has been modified from an earlier version.[17] In brief, the stop S_1 is focused on the front of the cornea, and the reflected light is refocused on the entrance slit of the spectrophotometer. The subject's head position is stabilized by a dental bite. The measurement area at the cornea is shown in Figure 1B. The dotted circle gives the illuminated disc (image of S_1) and the vertical dotted lines are the region sampled by the entrance slit of spectrophotometer. The sampled region is given by the vertical rectangle (solid line).

The original equipment[17] has been modified in the following ways: First, an improved spectrophotometer is used, including a SpectraPro-150 imaging spectrograph (Acton Research, Acton, MA), a Hamamatsu (Bridgewater, NJ) S5769–1006 CCD (charge-coupled device) Image Sensor, and an ST-133 CCD interface controller with Winspec version 1.6.1 Software (Princeton Instruments, Trenton, NJ). Advantages of the new system include lower noise level, greater dynamic range, ability to record at longer wavelengths, and interchangeable gratings for low- or high-resolution spectra. A second modification is the use of an uncoated, crown-glass, plano-convex lens for the calibration of reflectance (Fig. 1C). Reflection from the front surface of this "reference lens" returns along the axis of the optical system, but the lens is slightly rotated so that reflection from the rear surface is deflected to the side. Radius of curvature of the front surface is 7.75 mm, thus approximating that of the cornea. A third modification is the method of aligning the eye in three dimensions. The image of S_1 at the cornea is reimaged on a WAT-502A (Watec, Yamagata-Ken, Japan) videocamera by L_4, giving the left-hand spot on a video monitor (Fig. 1D, "focus"). When this spot is focused by axial motion of L_2, S_1 is focused on the cornea. Stop

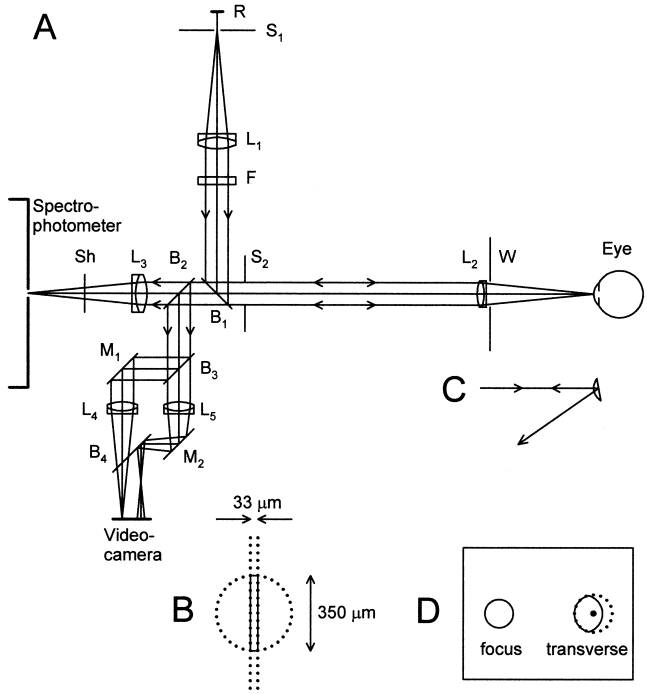

FIGURE 1. Measurement system. (**A**) Optical system (not to scale). R, ribbon filament source driven from a stabilized power supply; S_1 and S_2, circular stops; L_1 to L_5, lenses; F, OG550 filter; B_1 and B_2, glass plate beamsplitters; B3 and B4, mirror-type beamsplitters; W, white screen surrounding L_2; Sh, Shutter; M_1 and M_2, mirrors. (**B**) Measurement area at the cornea. (**C**) Use of the "reference lens" for the calibration of reflectance. (**D**) Video display for eye alignment.

S_2 is focused at the center of curvature of the cornea, and so, when the eye is aligned, the reflected light forms an image superimposed on S_2: this is then focused onto the videocamera by L_5, forming the right-hand spot (dotted circle) in Figure 1D ("transverse"). A dot is marked at the center of this spot to aid alignment. When the eye is misaligned laterally or vertically, the reflected image no longer superimposes on S_2, so that, for example, lateral misalignment gives the appearance indicated by the solid curve of the right spot in Figure 1D. Coarse alignment is achieved by movement of the dental bite and by observing the spot on the front of the cornea and its reflection onto the screen W; fine alignment is by small eye movements using the video display. A final modification is the addition of a Schott (Duryea, PA) OG550 filter, F in Figure 1A, which cuts off wavelengths below 550 nm, thus avoiding contamination of the recorded (first-order) spectrum by the second-order spectrum. As noted previously,[17] retinal irradiance was below the maximum permissible exposure for continuous viewing ($>10^4$ seconds) for both thermal and photochemical effects. Warming of the tear film by the measurement beam was calculated to be less than 0.3°C.

The spectrograph detector is an array of 1024 columns (wavelengths) × 64 rows. In "array-mode," the photoelectric charges from all 65,536 elements are read into the computer and stored on disc; the shutter, Sh, was used in this mode. In "binning mode," the 64 charges of each column (wavelength) are "binned" (added electrically) before being read; this mode is faster, but has a lower signal-to-noise ratio. The shutter was removed for this mode. *Low-resolution* spectra were obtained with a 300 grooves/mm grating, giving a spectral range of 562 to 1030 nm. These spectra are suitable for layers of up to 100 μm. The angular width of the illuminating cone at the cornea should be limited because of the effect of the $\cos(\phi')$ term in Equation 1. The diameter of S_2 was 10 mm, and the semi-angle of the illuminating cone was 4.8° (focal length of L_2 was 60 mm). *High-resolution* spectra used a 1200 grooves/mm grating with wavelength ranges of 760 to 836 nm or 865 to 931 nm. The diameter of S_2 was reduced to 3.2 mm, giving a semi-angle of 1.5° at the cornea. These spectra are suitable for layers of up to 1000 μm.

Data processing is illustrated in Figure 2. Empirically, it was found that the following steps, incorporated into a C program, provided satisfactory analysis. Step 1: Recorded spectra from the eye and from the reference lens were read from disc, and, for array-mode, the data from the 64 elements at each wavelength were added. Wavelength was converted to its reciprocal: wave number, χ. Figure 2A shows typical recorded spectra from the eye, $V(\chi)$, and from the reference lens, $V_L(\chi)$. Response units are 10^6 electrons per wavelength sample. Step 2: Spectra were corrected for small nonlinearities of the photodetector at each wavelength, giving corrected values $V'(\chi)$ and $V_L'(\chi)$. Step 3: Figure 2B illustrates the derivation of the reflectance spectrum of the eye,

$$r(\chi) = r_L(\chi)\ V'(\chi)/V_L'(\chi), \qquad (2)$$

where $r_L(\chi)$ is the reflectance of the reference lens, which was derived from Fresnel's equation.[12] Step 4: The sloping baseline of the reflectance spectrum (due to the lipid layer[9,15]) was fit by the Marquardt[19] method with the function

$$p(\chi) = [A + B\chi + C\chi^2 + D\chi^3][1 + Ev(\chi)][1 + Fb(\chi)], \qquad (3)$$

where *A, B, C, D, E,* and *F* are adjusted to provide a least squares fit. $v(\chi)$, $b(\chi)$ are derived from changes in the reflection spectra from the reference lens, with vertical and lateral displacement, respectively; their inclusion in Equation 3 provides a modest improvement to the accuracy of fit. In the fitting program, more weight was given to wavelengths with greater photodetector response (Fig. 2A). The resulting fit, $p(\chi)$, is shown by the dashed line in Figure 2B. Step 5: The fractional deviation of the reflectance from this fit, that is, $[r(\chi) - p(\chi)]/p(\chi)$ is shown by the black curve in Figure 2C. Step 6: This deviation was then reexpressed as a function of $\alpha = 2n\chi$, where n is the refractive index of the layer of interest. The refractive indices at 588 nm for tears[20] and cornea[21] were taken as 1.337 and 1.376, respectively, and their dispersion constant[12] was assumed to be the same as for water. A Fourier analysis of this spectrum as a function of α was then performed and is shown in Figure 2E. (Subtraction of $p(\chi)$ in step 5 improves the Fourier transform by reducing artifacts due to steps at the ends of the spectrum). Interference between reflections from two surfaces gives rise to a peak in the Fourier transform whose frequency corresponds to the thickness, t, of a layer (or more precisely, the depth of the second surface behind the air surface). This is shown by rewriting Equation 1 for normal incidence, that is,

$$m = 2n\chi t = \alpha t.$$

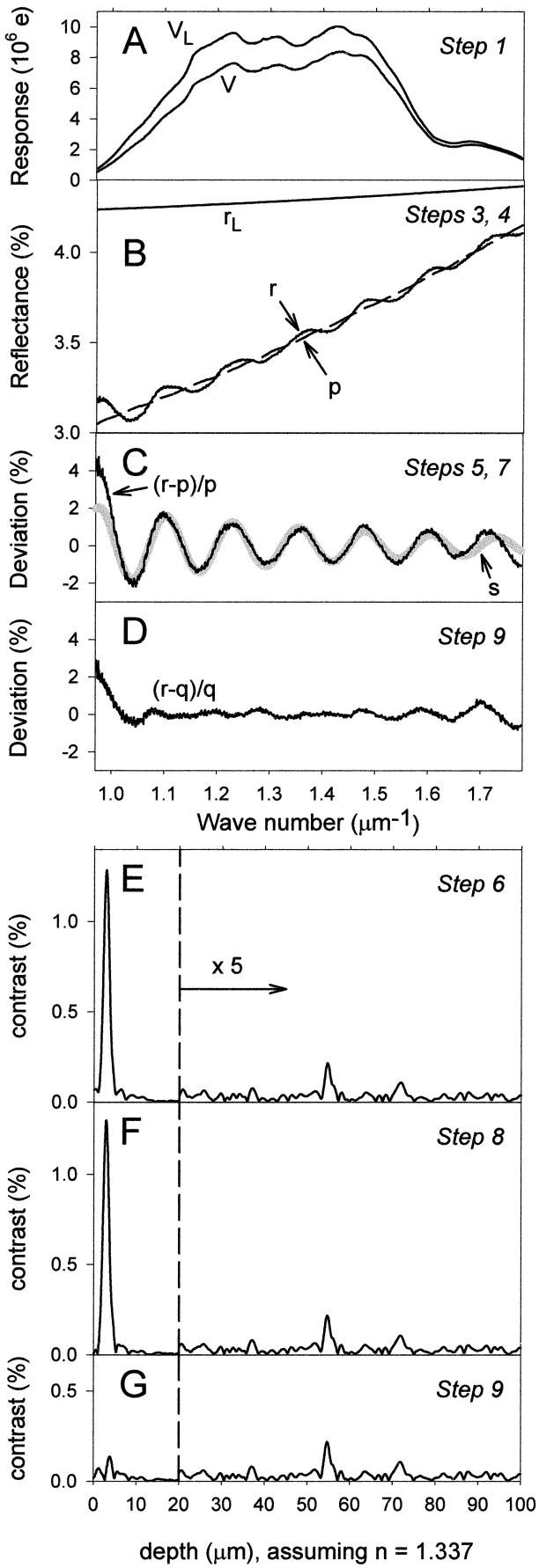

Thus, the frequency of the corresponding peak (number of cycles per unit of α) is given by

$$dm/d\alpha = t.$$

Unless otherwise noted, a Hann window was used to reduce the side lobes associated with large peaks, such as that near 3 μm.[19] Step 7: The depth of the largest peak from step 6 was used as a starting value (for T in Eq. 5 below) for a second Marquardt fit to $r(\chi)$ with the function

$$q(\chi) = s(\chi)\, p'(\chi), \tag{4}$$

where

$$s(\chi) = [1 + G \cos(2\pi T\alpha + H) \exp(-J\chi)], \tag{5}$$

and $p'(\chi)$ is given by Equation 3 (but with new constants A through F). A, B, C, D, E, F, G, T, H, and J are adjusted to provide a least squares fit. $p'(\chi)$ is found to be similar but not identical with $p(\chi)$. The $\cos(2\pi T\alpha + H)$ term gives the "spectral oscillations," whereas the decay term, $\exp(-J\chi)$, is empiric, providing a better fit to the spectrum.[17] The function, $s(\chi)$, is shown as the thick gray curve in Figure 2C. T is a new estimate of thickness, which generally has better repeatability than estimates from Fourier analysis. Values of thickness, T, corresponding to different peaks, can be obtained by limiting the Fourier analysis in step 6 to different thickness ranges; for example, for a range 20 to 100 μm in Figure 2E, the peak near 55 μm would be studied. Step 8: The fractional deviation of reflectance from p', that is, $[r(\chi) - p'(\chi)]/p'(\chi)$ is calculated and a second Fourier analysis is performed resulting in Figure 2F. Typically this Fourier transform is found to have somewhat smaller artifacts than the original transform (Fig. 2E). Step 9: The fractional deviation of reflectance from the overall fit, q, that is, $[r(\chi) - q(\chi)]/q(\chi)$ is calculated and is shown in Figure 2D. Another Fourier analysis is then performed, resulting in Figure 2G. This eliminates or reduces the peak in the Fourier transform near T, so that nearby weaker peaks may be studied better. In summary, the least squares fit of step 7 gives the best estimate of thickness, the Fourier transform of step 8 indicates the presence of interference from surfaces at different depths behind the air surface, whereas the transform of step 9 allows study of interference peaks near a major peak.

Wavelength calibration was performed by recording spectra after replacing the ribbon filament lamp with a low-pressure mercury/xenon light source (ML-900; Electro Technic Prod-

FIGURE 2. Data processing of data from a 24-year-old white man. (**A**) Recorded spectra from the eye, V, and from the reference lens, V_L. (**B**) The reflectance of the eye, r, is derived from the reflectance of the reference lens, r_L, and the recorded spectra in (**A**). The sloping baseline, due to the lipid layer of the tears, has been fitted by the function P (Eq. 3). (**C**) The *black curve* is the difference between the reflectance of the eye and the sloping baseline in (**B**). The *gray curve* is the fit to the spectral oscillations (s). (**D**) Deviation of the reflectance of the eye from the final fit. (**E**) Fourier transform of the *black curve* in (**C**). (**F**) Final Fourier transform. (**G**) Fourier transform of curve in (**D**), that is, after subtracting the main spectral oscillations.

ucts, Chicago, IL). For low-resolution spectra, the wavelengths of 12 spectral lines between 690.8 and 1014.0 nm were fitted by a cubic function of column number (1–1024). All points were within 0.1 nm of the calculated value. For high-resolution spectra, calibration of spectrometer geometric information using Winspec software was used. Thickness calibration was checked (after replacing the ribbon filament bulb) using an interferometer (OS-9255A; Pasco, Roseville, CA) whose micrometer was calibrated by counting 1000 fringes from a helium-neon laser. For a low-resolution spectrum, the interferometer was used in the Michelson mode[12] and placed to reflect the parallel beam through S_2 (Fig. 1A). For path differences between the two arms of the Michelson interferometer varying from 1.6 to 123 μm, a plot of measured thickness (from step 7 above) versus path difference gave a slope of 1.0046 and $r^2 = 0.999977$. For a high-resolution spectrum, the Fabry-Perot mode[12] was used and the interferometer was placed between F and B_1 in Figure 1A. For air gaps in the Fabry-Perot interferometer from 27 to 842 μm, the corresponding slope was 0.9935 and $r^2 = 0.999991$. These results indicate that thickness estimates were typically accurate to within 1%.

Procedure

Experiments were approved by our institutional review board and the tenets of the Declaration of Helsinki were followed. Informed consent was obtained from each subject.

A main experiment and several control experiments were performed. For the main experiment, low-resolution spectra were obtained using the slow "array-mode" of spectral readout. After the eye was aligned, the subject was asked to blink, and the reflection spectrum was recorded 2 seconds after the blink, with a 1-second exposure. Six normal subjects (3 men, 3 women; age range, 23 to 45 years; mean age, 32 years) and two subjects with dry eye symptoms (fluorescein break up time <10 seconds) took part in this experiment. Six spectra were obtained from the right eye of each subject. Average temperature and humidity were 26°C and 72%, respectively. Summary plots are given for only the normal subjects, but individual results from the dry eye subjects are included to illustrate certain findings.

The following control experiments were performed. (1) The time course of thickness changes was measured in six subjects. Low-resolution spectra were obtained using the fast "binning" spectral read out. In some experiments, the recording time was 20 seconds, and the subject was asked to blink approximately 1 second after the start of the recording; spectra were obtained every 27.5 ms. Two of the authors, who had exceptionally long break up times, kept their eyes open for 6 minutes without blinking while the time course of thickness change was measured (sampled every 0.525 seconds). (2) The main experiment was repeated in three subjects interspersed with trials during which the luminance of the measuring light had been reduced by a factor of 10. (3) The main experiment was repeated in three subjects, with the measurement area at the cornea reduced to 33 × 35 μm by using a narrow horizontal slit for S_1. (4) High-resolution spectra were obtained in six subjects using binning mode.

Statistical analysis was performed with Minitab 12 for Windows (State College, PA). $P < 0.05$ was considered to be statistically significant.

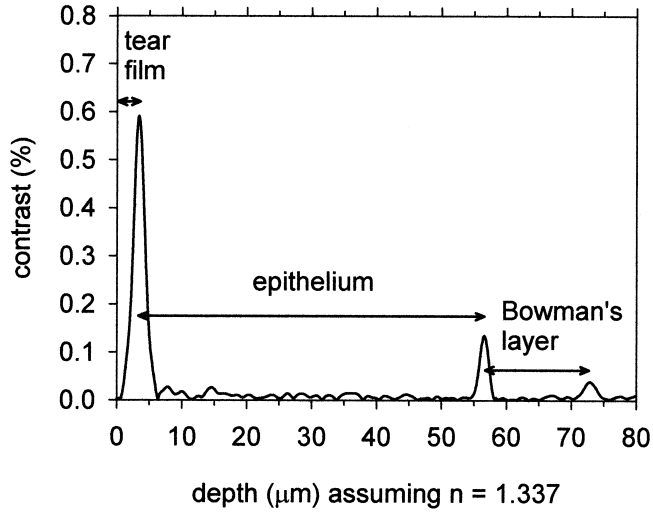

FIGURE 3. Fourier transform of reflection spectrum for a 58-year-old white man. An interpretation of depth ranges corresponding to the tear film, the epithelium, and Bowman's layer is given.

RESULTS

Main Experiment

Analysis of a typical low-resolution spectrum is shown in Figure 2 (see Methods). The (second) Fourier transform derived from the reflection spectrum is shown in Figure 2F. The largest peak, of contrast 1.3%, occurs at a depth of 2.9 μm behind the air surface; in the depth range above 20 μm (which includes the values obtained by Prydal et al.[6]) the largest peak, of contrast 0.043%, is at 54.8 μm, and there is a smaller peak, of contrast 0.021%, at 71.9 μm.

Figure 3 shows the Fourier transform of a spectrum for a subject who shows particularly large peaks in the range above 20 μm. (This subject had dry eye symptoms, but this probably does not limit the generality of the findings because the position of the major peaks are very close to those in Fig. 2.) In this subject, the largest peak, of contrast 0.59%, is at a depth of 3.4 μm; the next largest, of contrast 0.14% is at 56.6 μm; and the third largest, of contrast 0.039% is at a depth of 72.9 μm. These three peaks will be called the "3-μm peak," the "55-μm peak," and the "70-μm peak," corresponding to the approximate location of the peaks. A possible interpretation of these Fourier transforms is that the 3-μm peak corresponds to the reflection from the front of the epithelium, the 55-μm peak corresponds to the reflection from the back of the epithelium, and the 70-μm peak is from the back of Bowman's layer. Corresponding thicknesses of the tear film, epithelium, and Bowman's layer are indicated in Figure 3. If this interpretation is correct, the thickness of epithelium and Bowman's layer should be corrected for their respective refractive indices[21] (this is considered further in the Discussion).

Figure 4A is a plot of the contrast of the largest peak in the range 0 to 100 μm as a function of its depth, for all 36 spectra in 6 normal subjects. Each symbol corresponds to a different subject. All peaks were in the depth range 1.7 to 4.7 μm, that is, 3-μm peaks. Average depth was 2.7 ± 0.4 μm (SD between subjects) and average contrast was 0.98%. A significant difference between subjects was found by the Kruskal-Wallis test

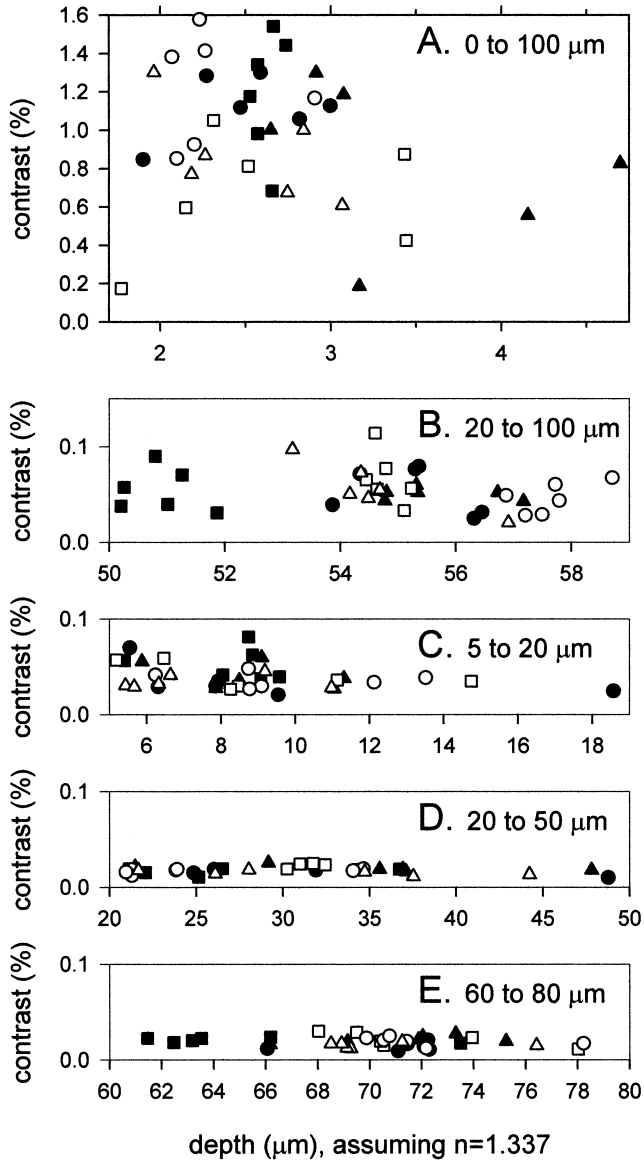

FIGURE 4. The contrast of the largest peak in 5 depth ranges, as indicated, plotted as a function of depth, for 36 spectra from 6 normal eyes. Each *symbol* corresponds to a different subject.

($P < 0.05$), indicating that these peaks are probably not artifacts of the equipment (further evidence for this is presented later).

Figure 4B is a similar plot for the range 20 to 100 μm. (Note that the contrast scale has been enlarged five times in Figs. 4B to 4E compared with Fig. 4A.) All peaks were in the depth range 50 to 59 μm, that is, 55-μm peaks. Average contrast was 0.055%. A significant difference between subjects was found by the Kruskal-Wallis test ($P < 0.001$), indicating that these peaks were recorded from the subject's eye and were not noise or artifacts of the equipment. None of the peaks in Figure 4B were in the range given by Prydal et al.[6]

Figure 4C shows the largest peaks in the range 5 to 20 μm, including the values of 10 to 12 μm of Danjo et al.[16] The average contrast was 0.040%, that is, only approximately 4% of the contrast of the 3-μm peaks in Figure 4A. No significant difference between subjects was found by the Kruskal-Wallis test. Figure 4D shows the largest peaks in the range 20 to 50 μm, including the values of Prydal et al.[6] The average contrast was 0.017%, that is, only approximately 2% of the contrast of the 3-μm peaks in Figure 4A. No significant difference between subjects was found by the Kruskal-Wallis test.

Figure 4E shows the largest peaks in the range 60 to 80 μm, which should presumably include the 70-μm peaks of Figures 2 and 3. The Kruskal-Wallis test did not show a significant difference between subjects. However, the eye represented by solid squares, which gave the six shallowest depths in Figure 4B (55-μm peaks), also gave the four shallowest depths in Figure 4E (70-μm peaks). This is expected if the 55- and 70-μm peaks correspond to reflection from the front and back of Bowman's layer, respectively, so that an eye with a thin epithelium and hence a shallow 55-μm peak (thickness of tear film + epithelium) would tend to have a shallow 70-μm peak (thickness of tear film + epithelium + Bowman's layer). A test of this proposal is shown in Figure 5A, where the depth of the largest peak in the range 60 to 80 μm (Fig. 4E) is plotted against the depth of the 55-μm peaks (Fig. 4B). The small symbols are the data from the main experiment. A significant positive correlation, $P < 0.001$, between the two values is found by the Spearman rank-order test. No correlation would be expected if the 70-μm peaks were an artifact of the equipment or quantum noise or a combination of both. The regression line fitted through all the data points is shown and has a slope of 1.23, which is not significantly different from 1; this is consistent with the interpretation that the difference between the 70- and the 55-μm peaks is the thickness of Bowman's layer, which is similar in all the subjects. Figure 5B is a plot of the depth difference between the 70- and the 55-μm peaks as a function of the depth of the 55-μm peak. Two data points, an open and a solid square, lie above the main distribution of data points and perhaps represent reflection from keratocytes. Omitting these two data points, the average difference between the 70- and 55-μm peaks, which is interpreted as the thickness of Bowman's layer, is 15.0 $\pm$ 1.3 μm (SD between subjects). The large symbols in Figure 5 are median values from two repeat sets of spectra for each of three subjects. The correlation between the 55- and 70-μm peaks in Figure 5A is consistent with that of the main experiment.

In conclusion, the results of the main experiment do not support values of human tear film thickness found by previous interferometric studies.[6,16] Weak interference effects are found for depths near 55 and 70 μm, which may correspond to reflections from the back of the epithelium and of Bowman's layer. A relatively strong interference effect is found for a surface at a depth of approximately 3 μm beneath the air surface, which may correspond to the epithelial surface. Thus, the thickness of the tear film would be approximately 3 μm. The following experiments were performed to help elucidate the nature of this layer.

Control Experiments

If the 3-μm layer is associated with the tear film, rather than being an artifact of the equipment, it should be systematically altered by blinking. Figure 6 confirms this prediction. Figure 6A shows the depth of the 3-μm layer recorded every 27.5 ms over a 20-second time period, using the rapid binning mode of the spectrograph detector. The subject was asked to blink

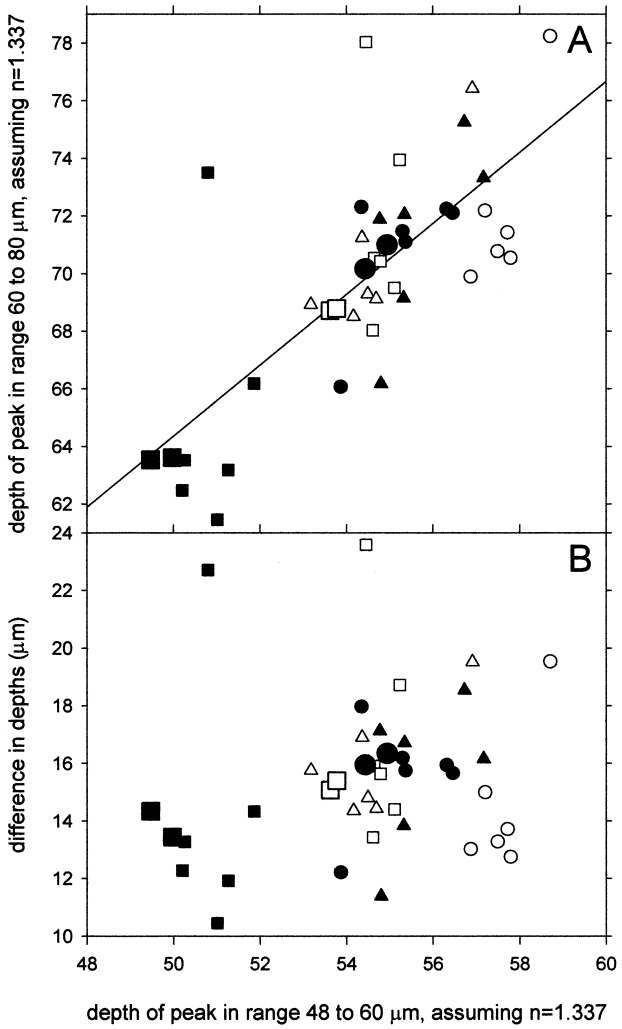

FIGURE 5. (**A**) Depth of the largest peak in the range 60 to 80 μm (70-μm peak) as a function of the depth of the largest peak in the range 48 to 60 μm (55-μm peak). Each *symbol* corresponds to a different subject. *Small symbols* are from individual spectra from the main experiment. A regression line has been fit to these data. *Large symbols* are median values from two repeat experiments for three of the subjects. (**B**) Plot of the difference between the 70- and 55-μm peaks as a function of the depth of the 55-μm peaks. This difference is interpreted as the thickness of Bowman's layer.

approximately 1 second after the start of the recording and then to keep her eyes open for the remaining 19 seconds. During the blink, the lid scatters the measuring beam diffusely, so less light is reflected back to the spectrograph than from the eye; thus, the timing of the blink is given by the drop in reflectance seen in Figure 6B. The blink causes the depth of the layer to jump from approximately 2.4 to 3.9 μm; it then decays rapidly in approximately 1 second to approximately 2.7 μm, followed by a slow decay to approximately 2.3 μm over the remaining 18 seconds. Thus, the 3-μm layer is associated with the subject's eye and is not an artifact of the equipment.

The possible contribution of reflex tears in response to the measurement light was assessed by reducing the luminance of the measurement beam by a factor of 10. For each of three normal subjects, 6 spectra at the standard intensity were followed by 12 spectra using the reduced intensity, followed by an additional 6 at the standard intensity; this order of presentation was used to reduce the effect of any steady drift in tear thickness during the measurements. Overall mean thickness at the standard and reduced intensities were 2.77 and 2.94 μm, respectively. There was no significant difference between these values, nor were there any significant differences between results for standard and reduced intensities for any of the subjects.

Evidence for the effects of reflex tears on the 3-μm layer is presented in Figure 7, which shows the variation of the depth of this layer for one subject when he held his eye open for 6 minutes without blinking. It is seen that the layer thinned steadily for about the first minute from approximately 3 μm down to 2 μm but then increased to a peak of nearly 5 μm before decaying back to approximately 2 μm. He afterward reported that his eye felt some irritation during the early part of the measurement, but the irritation then disappeared. Both the measurements and the subject's report can be explained by reflex tears, stimulated by the early irritation, and drifting down the cornea to cause thickening after the first minute. This presumably caused the relief of irritation. For another subject, the depth increased to a maximum of approximately 9 μm, which is the highest value that we have observed. In conclusion, our studies indicate that reflex tears do not contribute to the 3-μm layer, measured in the conditions of the main experiment. Reflex tears may thicken this layer up to approximately 9 μm.

A possible reason why our results do not confirm those of Danjo et al.[16] is that they used a measuring spot size of 30 μm, whereas our measuring area was larger, a vertical rectangle of

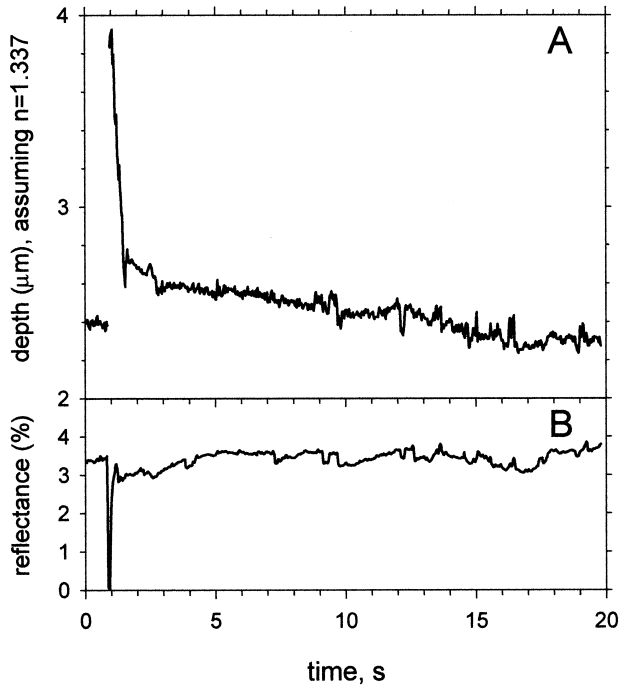

FIGURE 6. (**A**) Depth of the 3-μm layer, for a 29-year-old white woman, measured over a 20-second period. The subject was asked to blink approximately 1 second after the start of the recording. (**B**) Reflectance from the eye (at the central spectral wavelength, 800 nm) shows the timing of the blink (drop in reflectance).

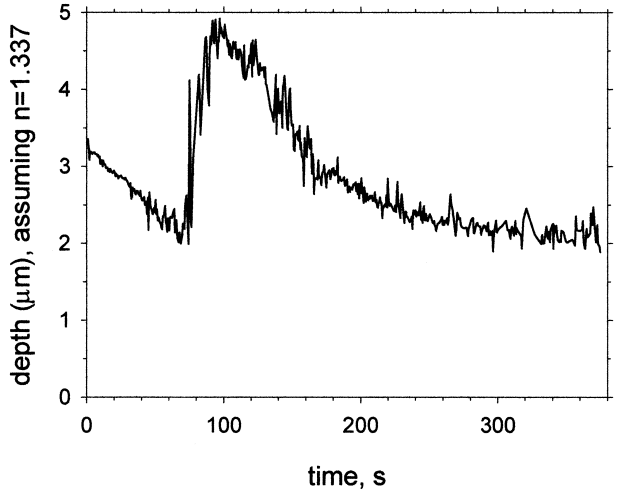

FIGURE 7. Variation in the depth of the 3-μm layer for one of the authors (a 31-year-old white man) when he held his eye open for approximately 6 minutes without blinking.

33 × 350 μm (Fig. 1B). We therefore repeated the main experiment with a comparable measuring area: 33 × 35 μm; 24 spectra were measured in each of three normal subjects. Figure 8 summarizes the findings as in Figure 4. In Figure 8A, which shows the largest peak in the complete range, 0 to 100 μm, 71 of 72 peaks lay in the range 1.6 to 5.8 μm, and their average contrast was 1.3%; one peak was at 54.2 μm. In Figure 8B, which shows the largest peak in the range 20 to 100 μm, 71 of 72 peaks lay in the range 48 to 57 μm, with an average contrast of 0.19%; one peak was at 70.0 μm. In Figures 8C and 8D, corresponding to the ranges 6 to 20 μm and 20 to 48 μm, respectively, average contrasts were 0.060% and 0.043% and so were only approximately 5% and 3% of the contrast of 3-μm peaks in Figure 8A. Figure 8E is for the range 60 to 80 μm, and so includes 70-μm peaks. The Kruskal-Wallis test for differences in depth values between subjects was significant for Figures 8A, 8B, and 8E ($P < 0.001$ in each case) but was not significant for Figures 8C and 8D.

If the relatively strong spectral oscillations from the 3-μm layer correspond to interference from the *front* of the cornea, one might expect to find oscillations of similar contrast from the *back* of the cornea. This prediction was tested using high-resolution spectra. Figure 9 shows pairs of Fourier transforms from four high-resolution spectra. For each spectrum, the upper thick curve gives the transform of the spectrum corresponding to Figure 2F, whereas the lower thin curve is the transform after subtracting the main spectral oscillations as in Figure 2G (contrast scale enlarged five times). Curves have been shifted vertically for clarity. The top two pairs of spectra were from one subject, whereas the bottom two pairs were from two other subjects. As predicted, strong "primary" peaks are observed with contrasts of up to 2.8% (top spectrum: the highest contrast from 120 high-resolution spectra in six subjects). Subject means ranged from 489 to 531 μm, with an overall mean of 511 ± 19 μm (SD between subjects).

Do the primary peaks correspond to reflection from the back of the cornea rather than, say, from the front or back of Descemet's membrane? Some evidence is provided by analysis of the secondary (nonprimary) peaks shown in the thin curves of Figure 9. The secondary peaks, which are shallower than the primary peak, tend to be stronger than those that are deeper. This would be expected if the primary peak corresponds to the back of the cornea, so that shallower secondary peaks could correspond to reflections from the stroma and Descemet's membrane, whereas deeper peaks, corresponding to depths within the (nonreflecting) aqueous humor, would be only noise. To study this further, we analyzed 120 spectra from 6 subjects (mean age, 36 years) and found all secondary peaks with a signal-to-noise ratio greater than 4 (where "noise" was

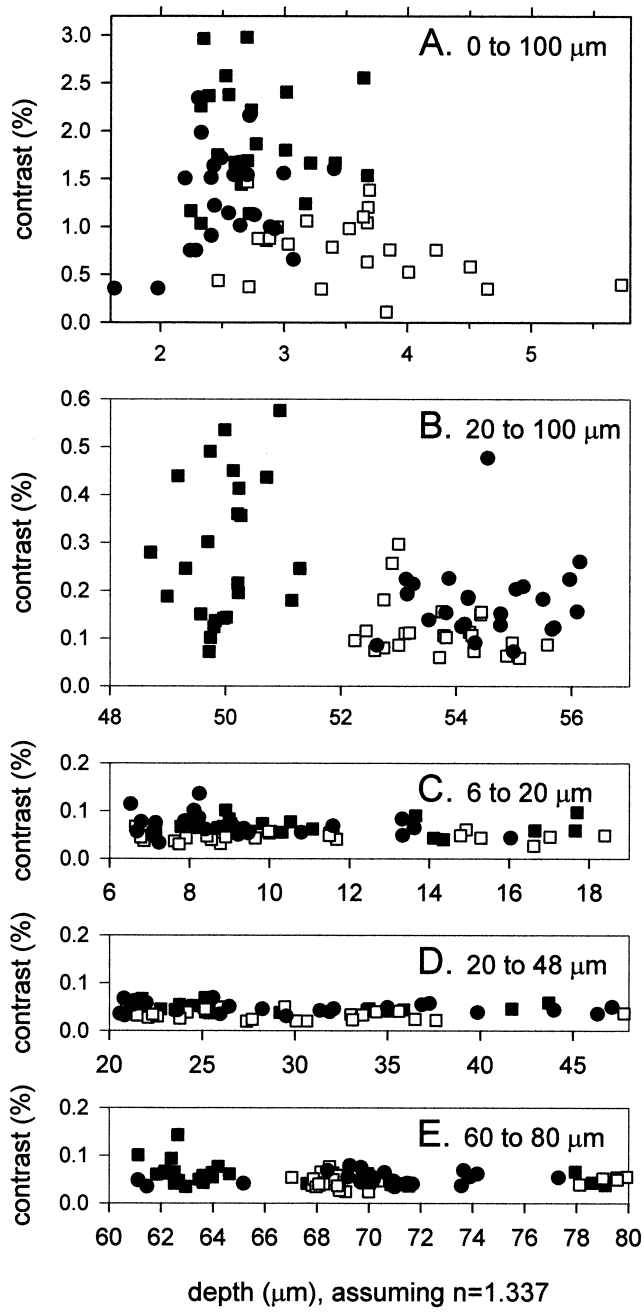

FIGURE 8. The contrast of the largest peak in 5 depth ranges plotted as a function of depth, for 72 spectra from 3 normal eyes. The size of the measurement area was reduced by a factor of 10 compared with the main experiment. Each *symbol* corresponds to a different subject.

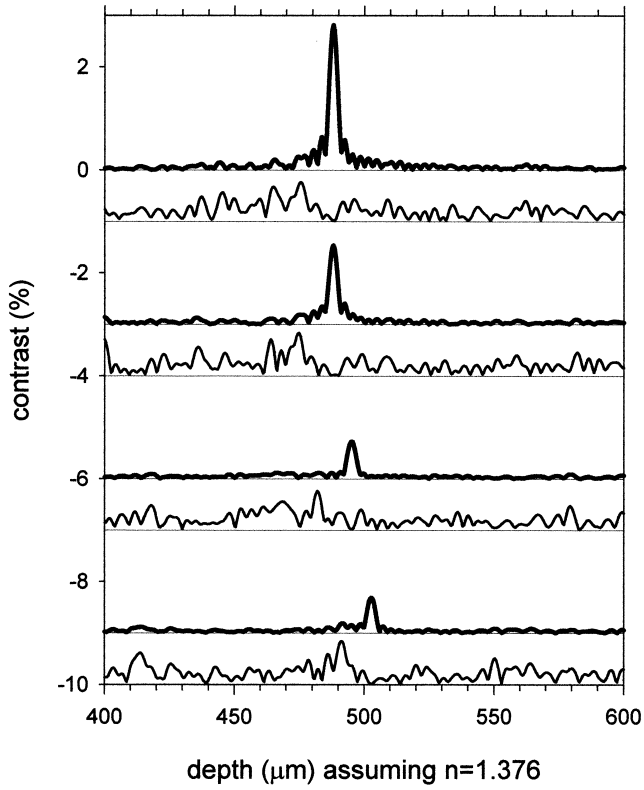

FIGURE 9. The *thick curves* are Fourier transforms of four high-resolution spectra. To improve resolution in depth, a square (rather than Hann) window was used for the Fourier transforms, and this contributed to the side lobes surrounding the primary peaks.[19] The *thin curves* are Fourier transforms of the spectra after subtracting the spectral oscillations corresponding to the primary peak (cf. Fig. 2**G**). *Curves* have been displaced vertically for clarity.

derived from the depth range 550 to 1000 μm). Figure 10A is a cumulative histogram of all such secondary peaks within ±100 μm of a primary peak; the vertical dashed line gives the position of the primary peak. Figure 10B is a "smoothed histogram" derived by summating Gaussian functions having SDs of 1 μm at the position of each secondary peak. Seventy-five secondary peaks were found up to 100 μm *shallower* than the primary peak, which is significantly more ($P < 0.001$, binomial distribution test) than the 3 (noise?) peaks that were found up to 100 μm *deeper* than it. This is the expected result if the primary peak corresponds to the back of the cornea.

DISCUSSION

Our results consistently show peaks at four different depths behind the air surface, namely, approximately 3, 55, 70, and 510 μm. The peaks near 3 μm (Figs. 2F, 3, 4A, 8A) and 510 μm (Fig. 9) have relatively high contrast. The peaks near 55 and 70 μm have lower contrast (Figs. 2F, 3, 4B, 4E, 8B, 8E).

These findings bear a striking resemblance to the observations of Li et al.,[22] who studied reflectance as a function of depth in the human cornea using confocal microscopy through focusing (CMTF). They also found four consistent peaks with the shallowest and deepest peaks, A and D, having considerably higher reflectance than the inner two, B and C. Using video pictures obtained from the confocal microscopy, they identified the four peaks in reflectance as follows: A, superficial epithelium; B, basal epithelial nerve plexus, corresponding to the basement membrane of the epithelium; C, anterior layer of keratocyte nuclei, behind Bowman's layer; and D, endothelium. They therefore interpreted distances between these peaks as the thickness of different layers as follows; AB, epithelial thickness (mean, 50.6 ± 3.9 μm; SD between subjects); BC, thickness of Bowman's layer (16.6 ± 1.1 μm); AD, corneal thickness (532 ± 19 μm). For our 33 × 350 μm measurement area and using published values for the refractive indices of epithelium (1.401), Bowman's layer (1.380), and stroma (1.376),[21] our findings are similar: epithelial thickness, 49.7 ± 2.2 μm (SD between subjects); Bowman's layer, 14.6 ± 1.4 μm; and cornea (after subtracting 3 μm for assumed tear film thickness), 508 ± 19 μm. Thus, our findings are consistent with those from CMTF, not only in the relative contrast or reflectances from the four peaks, but also in the separation between the peaks; our interpretation of the origin of the four peaks agrees with that of Li et al.[22]

If the high-contrast interference peak at a depth near 510 μm comes from the back of the cornea, this would support the proposal that the other high-contrast peak near 3 μm comes from the front of the cornea. But does the 510 μm peak really come from the back of the endothelium, or could it derive from one of the surfaces of Descemet's membrane? The fact that the deepest reflectance peak in CMTF corresponds to an image of endothelial cells,[22] similar to images seen in scanning electron micrographs, is consistent with an origin at the back of the endothelium. However, it is possible that this pattern of polygonal cells could correspond to the front of the endothe-

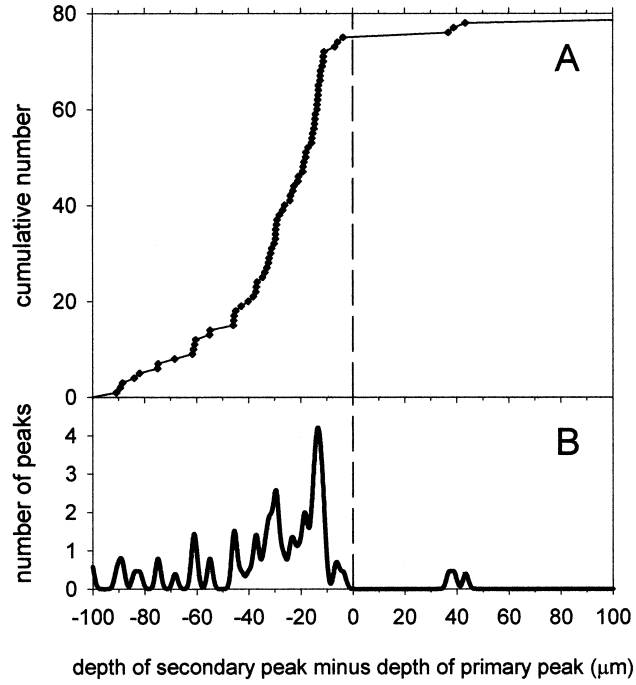

FIGURE 10. Depth of secondary peaks having a signal-to-noise ratio greater than 4, relative to depth of primary peaks, derived from 120 high-resolution spectra. The position of the primary peak is given by the *dashed line*. (**A**) Cumulative histogram; (**B**) smoothed histogram.

lium. Various observations make this alternative unlikely. First, when inflammatory cells in the aqueous humor settle on the endothelial surface, black spots are seen in the confocal microscopic image of the endothelium,[23] as would be expected if this image is from the back of the endothelium.

Additional evidence comes from the histograms of secondary peaks in Figure 10. As noted previously, there are many secondary peaks shallower than the primary peak, but few are deeper; this is to be expected if the primary peak corresponds to the back of the cornea. The endothelium is approximately 5 μm thick,[24] and Descemet's membrane is approximately 9 μm thick at the mean subject age of 36 years.[25] The maximum in the histogram of Figure 10B is at 13.4 μm, which is close to the combined thickness of endothelium and Descemet's membrane of approximately 14 μm. This is consistent with the proposal that the primary peak comes from the back of the endothelium. whereas the maximum in Figure 10B corresponds to the front of Descemet's membrane. In Figure 10, it is seen that there are three secondary peaks at approximately 5 μm shallower than the primary peak; these are consistent with reflections from the front of the endothelium if the primary peak corresponds to the back of the endothelium. Given that the reflectance of a surface depends on the difference in refractive index across that surface,[12] the finding that there are only three peaks near this depth could be explained if the refractive index of endothelial cells was close to that of Descemet's membrane. It may be noted that the refractive index of parts of monkey photoreceptors[26] varies from approximately 1.36 to 1.41, so that a value of refractive index of endothelium near that of the corneal stroma (1.376) is not unreasonable.

The 3-μm Peak

The effects of a blink on the thickness of the 3-μm layer, shown in Figure 6, show that this layer is not an artifact of the equipment. An interpretation of this recording is that the rapid decay after the blink corresponds to the redistribution of tear film associated with upward motion of the lipid layer,[3,27] whereas the slow decay corresponds to evaporation from the tear film.[28] The results of Figure 7 also help to demonstrate that the 3-μm layer is not an artifact.

What is the 3-μm layer? Spectral oscillations are generated by interference between the strong reflection from the air surface and a reflection from some deeper surface. The 3-μm layer is too thick to be the lipid layer,[9,15] but it could be the aqueous layer (plus the thin lipid layer), or it could be the complete thickness of the tear film. High contrast fringes can occur if the reflection from the deeper surface is relatively strong. By Fresnel's equation,[12] this will occur if there is a *large* change in refractive index across the surface; an additional condition for a strong reflection is that the step change in refractive index should be *sharp* compared with the wavelength of light. The refractive index step between the tear film[20] and the epithelium[21] is relatively large (approximately 0.064) and sharp, and so this interface would be expected to give a relatively strong reflection. However, at the aqueous/mucus interface, reflectance should be weak because of the small difference in refractive index between aqueous and mucus. This is because the concentration of mucin in mucus is relatively low (approximately 0.5–1%[29]), and thus the refractive index difference between mucus and aqueous tears should be small (approximately 0.0018 for a mucin concentration of 1%,[30] that is, only approximately 3% of the step at the tear/cornea interface). Additionally, it may be noted that mucin molecules can be as long as 3 μm,[31] so that the boundary between aqueous and mucus layers may be blurred over a distance comparable to the wavelength of light, again reducing the reflectance of this boundary. The conclusion is that interference from the aqueous/mucus interface should be weak compared with interference from the tear/corneal interface. If the 3-μm peak corresponds to the aqueous/mucus interface, then this should be much smaller than a peak at a greater depth, corresponding to the tear/corneal interface. This is inconsistent with our results; Figure 4 shows that the 3-μm peak is much larger than any other peak in the range up to 50 μm. It also seems improbable that any of the peaks seen in the 5- to 50-μm range in Figures 4C and 4D could come from the tear/cornea interface, because they are much smaller than the peaks from the cornea/aqueous humor interface in Figure 9. Finally, it may be noted that the mucus layer may extend, without discontinuity, from the corneal surface to the lipid layer[32]; in this case the 3-μm layer obviously could not be the aqueous layer. In summary, the finding that the 3-μm peaks in Figure 4 are the much larger than others up to 50 μm depth, is consistent with the proposal that the they come from the tear/corneal interface, implying that the thickness of the human tear film is approximately 3 μm. The fact that the 3-μm peaks are comparable in size to the primary peaks in Figure 9, which come from the cornea/aqueous humor interface, is also consistent with their coming from the tear/cornea interface.

We have not found a peak at a depth of less than 3 μm, which might correspond to the aqueous/mucus boundary (see Fig. 2G). As noted above, the refractive indices of mucus and aqueous layers would differ by only approximately 0.13%. Correspondingly, regardless of whether the tear film is mainly aqueous, is mainly mucus, has about equal thicknesses of both, or has a gradient of mucin concentration, the estimate of tear film thickness would be affected by only about this small percentage (cf. Eq. 1, which shows that calculated thickness, t, is inversely proportional to assumed refractive index, n).

Our analysis indicates similarities between interference effects from the anterior and posterior regions of the cornea. In Figure 3, it is proposed that the front surface of the cornea gives rise to a strong interference peak, whereas the internal boundaries between epithelium, Bowman's layer, and stroma give weaker peaks. A symmetrical explanation is proposed for interference peaks from the posterior layers shown in Figures 9 and 10. The strong, primary peak is interpreted as interference from the back surface of the cornea, whereas weaker, secondary peaks may occur at the internal boundaries between endothelium, Descemet's membrane, and stroma. Thus, for both the anterior and posterior regions of the cornea, the external surface may give stronger interference than the internal boundaries.

In conclusion, we interpret the 3-μm peak as coming from the front of the cornea, implying that the normal tear film thickness is approximately 3 μm; reflex tears can increase this thickness (Fig. 7). A thickness of 3 μm is comparable to that of the prelens tear film.[13,17] This thickness is considerably less than previous interferometric estimates using angle-dependent[6] and wavelength-dependent[16] fringes. It is probable that the 3-μm layer was too thin to be detected in those experi-

ments; Prydal et al.[6] note that 6 μm was the minimum thickness measurable by their method, whereas Danjo et al.[16] used a limited spectral range, which would make it difficult to detect relatively thin films. Regarding their reported thickness values, it is possible that thin films in the equipment (e.g., cement layers in doublet lenses) may have caused artifacts in both sets of measurements. (In our method, the effect of such artifacts was reduced by dividing the recorded spectrum by that from the reference lens [Eq. 2] and by the terms $v(\chi)$ and $b(\chi)$ in Eqs. 3 and 4). Additionally, in Danjo's experiment,[16] the spectrum was scanned over a 2-second period, which could cause artifacts due to eye movements and thinning of the tears during the spectral scan; we used a shorter (1 second) exposure and collected responses for all wavelengths simultaneously. In Prydal's experiment,[6] spatial noise from the laser source may have caused problems in detecting and analyzing fringes. An advantage of our method is its low noise level, so that fringes of below 0.1% contrast can be readily detected and analyzed (e.g., Fig. 3). It seems difficult to find an alternative explanation for Prydal's data, which showed thinning of his 40-μm layer after application of acetylcysteine; however, the reported results in humans are for only one subject, and an attempt to reproduce them was not convincing (D. Maurice, personal communication, 1999).

Regarding invasive methods, Mishima[7] reported measurements by two methods that gave an average thickness of 7 μm. One concern with these measurements is that they were performed in the rabbit, whose tear film may differ considerably from the human; for example, the interblink interval in the rabbit can be more than 300 seconds, compared with only approximately 7 seconds in the human.[33] An additional reservation about Mishima's first method, immersion of fine glass filaments in the tear film, is that the filament may indent the epithelium. Evidence for this is, first, that a transient indentation in the tear film can be seen after removal of the filament; second, that the filament is quite uncomfortable in the unanesthetized eye; and third, that when fluorescein is instilled after the experiment, a persistent, very fine, fluorescent line is seen in the epithelium (D. Maurice, personal communication, 2000). A reservation about Mishima's second experiment, fluorometry, is that the eye was proptosed and the tear film was washed away with saline containing fluorescein; it is not obvious that this saline film will have the same thickness as the normal tear film. A fluorometric estimate in the human of 4 μm[5] is closer to ours; however, the authors were interested in the effect of instilled agents and only, in passing, extrapolated their data to estimate tear film thickness, so this result may not be considered to be definitive. By applying an absorbent paper disc to the cornea,[8] human tear film thickness was estimated to be approximately 8 μm, which could be an overestimate if reflex tears were generated and/or if fluid was drawn from the tear film surrounding the disc or epithelium. Finally, theoretical predictions of fluid mechanics have been used to predict tear film thickness, yielding a mean value of 10.4 μm[34]; although the theory of the calculations is well established,[2] there are uncertainties in assumptions of the model (e.g., in the values of viscosity, surface tension, and upper eye lid velocity and in the assumption that the upper tear meniscus is not depleted during its upward motion) that could be the basis of the discrepancy between that estimate and ours.

Acknowledgments

The authors thank an anonymous editor, two referees and Sara L. Alvarez, Joseph T. Barr, Carolyn G. Begley, Tyson Brunstetter, Yukitaka Danjo, Marshall G. Doane, Richard A. Farrell, Jean-Pierre Guillon, James V. Jester, Stephen D. Klyce, Charles J. Koester, Donald R. Korb, David M. Maurice, Roswell R. Pfister, Jeremy I. Prydal, Clayton J. Radke, John M. Tiffany, Alan Tomlinson, and Karla Zadnik for advice and comments. Statistical advice was provided by Lisa A. Jones.

References

1. Wolff E. Mucocutaneous junction of lid-margin and distribution of tear fluid. *Trans Ophthal Soc UK.* 1946;66:291–308.
2. Wong H, Fatt I, Radke CJ. Deposition and thinning of the human tear film. *J Colloid Interface Sci.* 1996;184:44–51.
3. Brown SI, Dervichian DG. Hydrodynamics of blinking. *Arch Ophthalmol.* 1969;82:541–547.
4. Holly FJ. Formation and rupture of the tear film. *Exp Eye Res.* 1973;15:515–525.
5. Benedetto DA, Shah DO, Kaufman HE. The instilled fluid dynamics and surface chemistry of the tear film. *Invest Ophthalmol Vis Sci.* 1975;14:887–902.
6. Prydal JI, Artal P, Woon H, Campbell FW. Study of human precorneal tear film thickness and structure using laser interferometry. *Invest Ophthalmol Vis Sci.* 1992;33:2006–2011.
7. Mishima S. Some physiological aspects of the precorneal tear film. *Arch Ophthalmol.* 1965;73:233–241.
8. Ehlers N. The thickness of the precorneal tear film. *Acta Ophthalmol.* 1965;81:92–100.
9. King-Smith PE, Fink BA, Fogt N. Three interferometric methods for measuring the thickness of layers of the tear film. *Optom Vis Sci.* 1999;76:19–32.
10. Drexler W, Baumgartner A, Findl O, Hitzenberger CK, Sattmann H, Fercher AF. Submicrometer precision biometry of the human eye. *Invest Ophthalmol Vis Sci.* 1997;38:1304–1313.
11. Doane MG. An instrument for in vivo tear film interferometry. *Optom Vis Sci.* 1989;66:383–388.
12. Jenkins FA, White HE. *Fundamentals of Optics.* 4th ed. New York, NY: McGraw-Hill; 1974.
13. Guillon JP. Tear film structure and contact lenses. In: Holly FJ, ed. *The Preocular Tear Film in Health, Disease and Contact Lens Wear.* Lubbock, TX: Dry Eye Institute; 1986:914–939.
14. Green DG, Frueh BR, Shapiro JM. Corneal thickness measured by interferometry. *J Opt Soc Am.* 1975;65:119–123.
15. Olsen T. Reflectometry of the precorneal tear film. *Acta Ophthalmol.* 1985;63:432–438.
16. Danjo Y, Nakamura M, Hamano T. Measurement of the precorneal tear film thickness with a non-contact optical interferometry film thickness measurement system. *Jpn J Ophthalmol.* 1994;38:260–266.
17. Fogt N, King-Smith PE, Tuell G. Interferometric measurement of tear film thickness by use of spectral oscillations. *J Opt Soc Am A.* 1998;15:268–275.
18. King-Smith PE, Fink BA, Fogt N, Kinney KK, Hill RM. Is the thickness of the tear film about 40 μm or about 3 μm? [ARVO Abstract]. *Invest Ophthalmol Vis Sci.* 1999;40(4):**S**544. Abstract nr 2876.
19. Press WH, Flannery BP, Teukolsky SA, Vetterling WT. *Numerical Recipes in C.* Cambridge, UK: Cambridge University Press; 1988: 542–547.
20. Craig JP, Simmons PA, Patel S, Tomlinson A. Refractive index and osmolarity of human tears. *Optom Vis Sci.* 1995;72:718–724.
21. Patel, S, Marshal J, Fitzke FW. Refractive index of the human epithelium and stroma. *J Refract Surg.* 1995;11:100–105.
22. Li HF, Petroll WM, Moller-Pedersen T, Maurer JK, Cavanagh HD, Jester JV. Epithelial and corneal thickness measurements by in vivo confocal microscopy through focussing (CMTF). *Curr Eye Res.* 1997;16:214–221.

23. Koester CJ, Roberts CW. Wide-field specular microscopy. In: Masters BR, ed. *Noninvasive Diagnostic Techniques in Ophthalmology.* New York: Springer-Verlag; 1990:99–121.
24. Beuerman RW, Pedroza L. Ultrastructure of the human cornea. *Microsc Res Tech.* 1996;33:320–335.
25. Murphy C, Alvarado J, Juster R. Prenatal and postnatal growth of the human Descemet's membrane. *Invest Ophthalmol Vis Sci.* 1984;25:1402–1415.
26. Sidman RL. The structure and concentration of solids in photoreceptor cells studied by refractometry and interference microscopy. *J Biophys Biochem Cytol.* 1957;3:15–30.
27. Benedetto DA, Clinch TE, Laibson MD. In vivo observation of tear dynamics using fluorophotometry. *Arch Ophthalmol.* 1984;102: 410–412.
28. Mishima S, Maurice DM. The oily layer of the tear film and evaporation from the corneal surface. *Exp Eye Res.* 1961;1:39–45.
29. Creeth JM. Constituents of mucus and their separation. *Br Med Bull.* 1978;34:17–24.
30. Barer R, Ross KFA, Tkaczyk S. Refractometry of living cells. *Nature.* 1953;171:720–724.
31. Dilly PN. Structure and function of the tear film. *Adv Exp Med Biol.* 1994;350:239–247.
32. Chen H-B, Yamabayashi S, Ou B, Tanaka Y, Ohno S, Tsukahara S. Structure and composition of the rat corneal tear film. *Invest Ophthalmol Vis Sci.* 1997;38:381–387.
33. Korb DR, Greiner JV, Glonek T, et al. Human and rabbit lipid layer and interference pattern observations. *Adv Exp Biol Med.* 1998; 438:395–398.
34. Creech JL, Do LT, Fatt I, Radke CJ. In vivo tear-film thickness determination and implications for tear-film stability. *Curr Eye Res.* 1998;17:1058–1066.